Appl Nanosci (2016) 6:461–466
DOI 10.1007/s13204-015-0462-2

REVIEW ARTICLE

Investigations of LBMO thin films deposited on different substrates by electron beam evaporation

Ch. Seshendra Reddy[1] · Ch. Ashoka Reddy[1] · A. Sivasankar Reddy[2] · P. Sreedhara Reddy[1]

Received: 4 May 2015 / Accepted: 23 May 2015 / Published online: 5 June 2015
© The Author(s) 2015. This article is published with open access at Springerlink.com

Abstract $La_{0.7}Ba_{0.3}MnO_3$ (LBMO) thin films were prepared on different substrates such as Si, MgO, and c-ZrO_2 substrates at substrate temperature 1023 K using electron beam evaporation technique for first time. Through optimizing the preparation condition, the better film uniformity of thickness, composition, and temperature was achieved. To find the influence of substrates, we studied the structural, compositional, morphological, and electrical properties of LBMO thin films. All the LBMO films exhibited a single phase and good crystallinity with no impurity phases. Films deposited on MgO have high temperature coefficient of resistance (TCR) value with low transition temperature (245 K). Better TCR (4.09 %/K) value at room temperature is observed in LBMO films deposited on Si substrate.

Keywords Structural · AFM · Substrates · Electrical · TCR

Introduction

Perovskite manganese oxides are well known because of their varieties of unique magnetic and electrical behaviors such as colossal magnetoresistance (CMR) (Kusters et al. 1989; Chahara et al. 1993; Jin et al. 1994; Helmolt et al. 1993) accompanied with a metal–insulator transition, electronic phase separation (Renner et al. 2005; Uehara et al. 1999; Renner et al. 2002; Antonakos et al. 2008; Hong et al. 2003; Wang et al. 2009), and strong coupling among spin, charge, orbital, and lattice degrees of freedom (Chen and Cheong 1996; Jirak et al. 2000). These materials have also aroused great interest because of the potential applications in devices such as read heads and sensors. Since most applications of CMR materials are in a form of film, it is important to study the factors that affect the properties of manganite films. Actually, numerous researches on strain effects in epitaxial manganite films have been reported since the discovery of CMR, in order to shed some light on such a strongly correlated electron system with multi-degree of freedom (Huang et al. 2009; Ovsyannikov et al. 2009; Sagdeo et al. 2008). While sophisticated deposition techniques like PLD (Jin et al. 1994; Goyal et al. 1997; Rajeswari et al. 1996) and MBE (Vas'ko et al. 1996) are highly successful in growing epitaxial thin films of manganites, other cost-effective deposition techniques with greater flexibility in terms of various deposition control parameters would be desirable. In order to realize a good sensor detectivity, high TCR values are warranted. Attempts have been made to fabricate uncooled detectors using semiconducting YBCO grown on silicon at low temperature and have met with considerable success (Shan et al. 1995). Such films are semiconducting at room temperature instead of the usual metallic ones grown at high temperatures on crystalline oxide substrates. CMR ($R_{1-x}A_xMnO_3$), R=La, A=Ca, Sr, Ba, which are at the focus of significant scientific activity over the past decade (Salamon and Jaime 2001; Tokura and Tomioka 1999), can also offer considerable tunability of their transport properties via control of cation stoichiometry and oxygen content. It is important to mention that crystalline films of manganites grown on single crystaloxide substrates at high temperature have been studied for uncooled and cooled detector applications. However, this approach yields

✉ Ch. Seshendra Reddy
seshu123reddy@gmail.com

[1] Department of Physics, Sri Venkateswara University, Tirupati 517502, India

[2] Department of Physics, V.S.U. P.G. Centre, Kavali 524201, India

positive TCR and is not technologically compatible with the existing silicon technology due to high film growth temperatures involved. In this work, LBMO films deposited on Si and single-crystal oxide substrates using electron beam evaporation technique.

Experimental

LBMO thin films deposited on different substrates such as Si, MgO, and c-ZrO_2 using electron beam evaporation, and the target was prepared using solid-state reaction method. Stoichiometric amounts of high purity (99.99 %) La_2O_3, $BaCO_3$, and MnO_2 powders were mixed, and the obtained single-phase powders were pelletized and sintered at 1373 K in air for 16 h. The distance between the substrate and the evaporation source was approximately 50 mm, and the substrate temperature was maintained at 1023 K by a resistance heater. The pelletized LBMO targets were heated by means of an electron beam collimated from the dc heated tungsten filament cathode, and the voltage and current were constant at 5 kV and 50 mA, respectively. The deposition parameters maintained during the preparation of LBMO films are given in Table 1. The structure of LBMO thin films was characterized by X-ray diffraction (XRD) with Cu Kα (0.154 nm) line as the radiation source. The elemental analysis of the films was carried using energy dispersive spectroscopy (EDS). The surface morphology was observed using atomic force microscopy (AFM). The electrical properties of the films were analyzed using standard four-probe method in the temperature range 213–333 K.

Results and discussions

Structural properties

The X-ray diffraction patterns of the films formed on different substrates are shown in Fig. 1. The peaks in the spectra of LBMO thin films deposited on Si, MgO, and c-

Table 1 Deposition parameters of LBMO thin films

Parameters	Values
The target to substrate distance	50 mm
Base pressure	1.3×10^{-5} mbar
Working pressure	2×10^{-4} mbar
Substrate temperature	1023 K
Evaporation time	15 min
Accelerating voltage	5 kV
Filament current	50 mA
Substrates	Si, MgO, c-ZrO_2

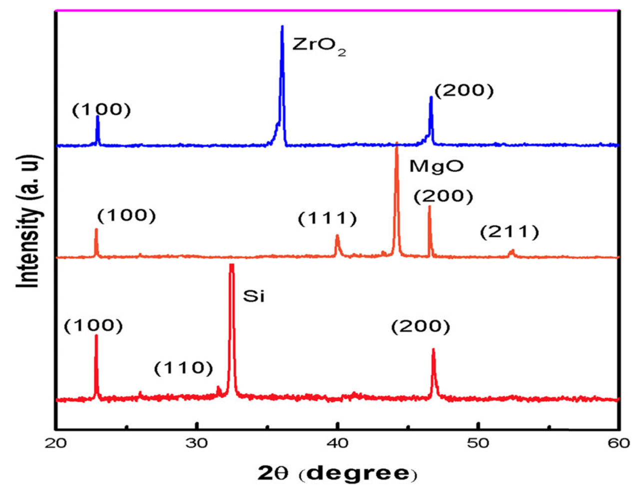

Fig. 1 X-ray diffraction patterns of LBMO films deposited on different substrates

Table 2 Crystalline size and lattice parameter values of LBMO thin films formed on different substrates

Substrate	Orientation (hkl)	Crystalline size (*d*) (nm)	Lattice parameter (*a*) (nm)
Si (100)	(200)	34	0.388
MgO (100)	(200)	39	0.394
c-ZrO_2	(200)	28	0.387

ZrO_2 substrates confirm the pseudo cubic structure. The absence of impurity peaks in the XRD patterns of all the films indicates that the films are single phase. The films prepared on Si substrate exhibited (100), (110), and (200) preferred orientations. The films prepared on c-ZrO_2 substrate exhibited (100) and (200) orientations, and the films prepared on MgO substrate exhibited (100), (111), (200), and (211) orientations. Furthermore, a small angular shift of the (100) and (200) peaks is observed with changing substrates. The crystallinity of LBMO films was determined from the full width at half maximum (FWHM) values of (200) diffraction peak. Since FWHM is one of the measurements of crystallinity, smaller FWHM values indicate the higher crystalline films. The crystalline size (L) of the films was calculated from the X-ray diffraction peak using the Scherrer's relation:

$$L = k\lambda/\beta\cos\theta, \quad (1)$$

where β is the full width half maxima (FWHM) of the XRD peaks after subtracting, θ is the Bragg angle, K is the practical factor (=0.89), and λ is the wavelength of Cu Kα radiation. The values of crystalline sizes given in Table 2 are found to be in the range from 28 to 39 nm. It is observed that the smallest one corresponds to the LBMO thin films deposited on c-ZrO_2 substrate. The lattice parameters of LBMO films formed on Si, MgO, and c-ZrO2 are 0.388,

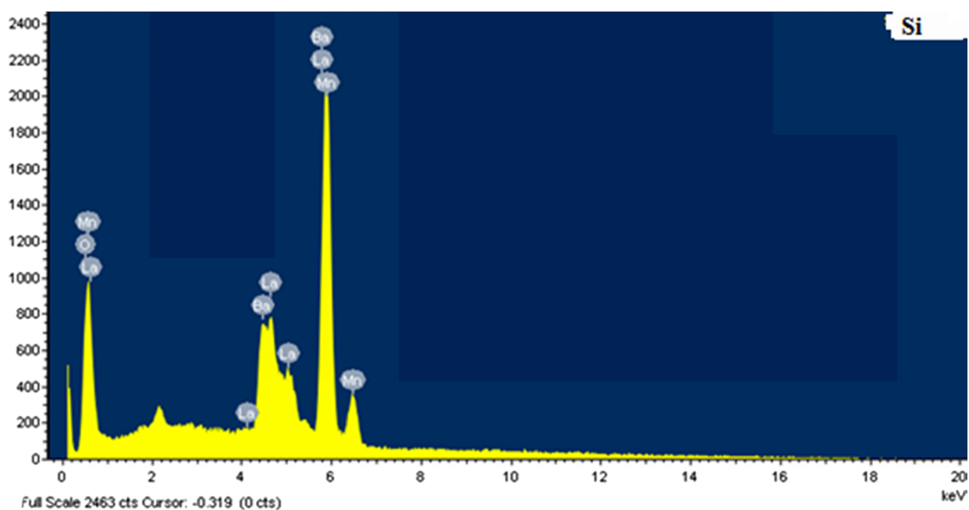

Fig. 2 EDS pattern of the LBMO film deposited on Si substrate

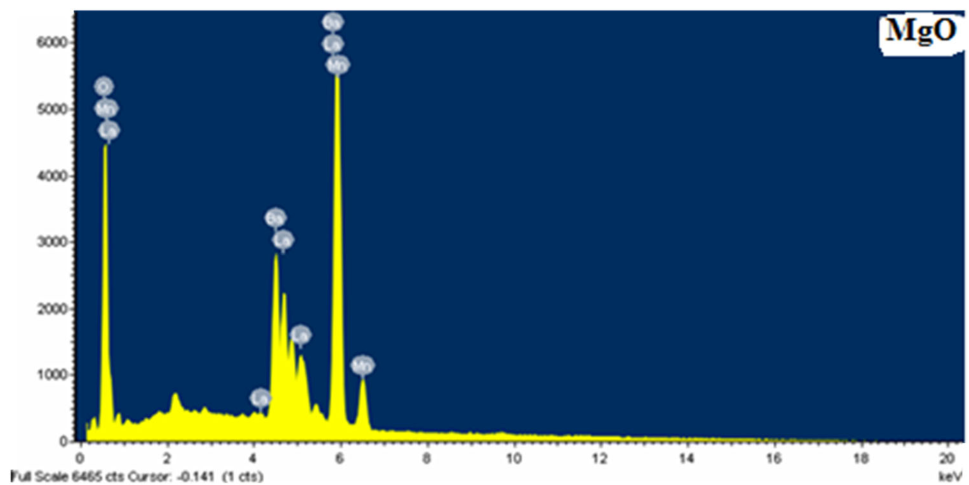

Fig. 3 EDS pattern of the LBMO film deposited on MgO substrate

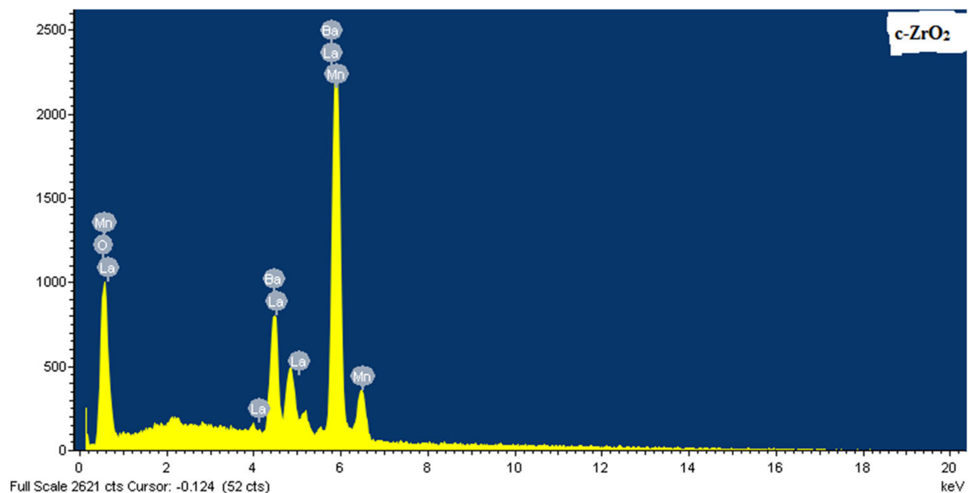

Fig. 4 EDS pattern of the LBMO film deposited on c-ZrO_2substrate

0.392, and 0.387 nm, respectively. Electronic properties of thin epitaxial films are influenced by the nature of the substrate which largely controls the film growth morphologies, defect structure, and the level of stress.

In general, if the difference between the lattice parameters of the film and substrate is within 1 ± 2 %, film growth takes place in a layer by layer mode accommodating the difference through expansion or

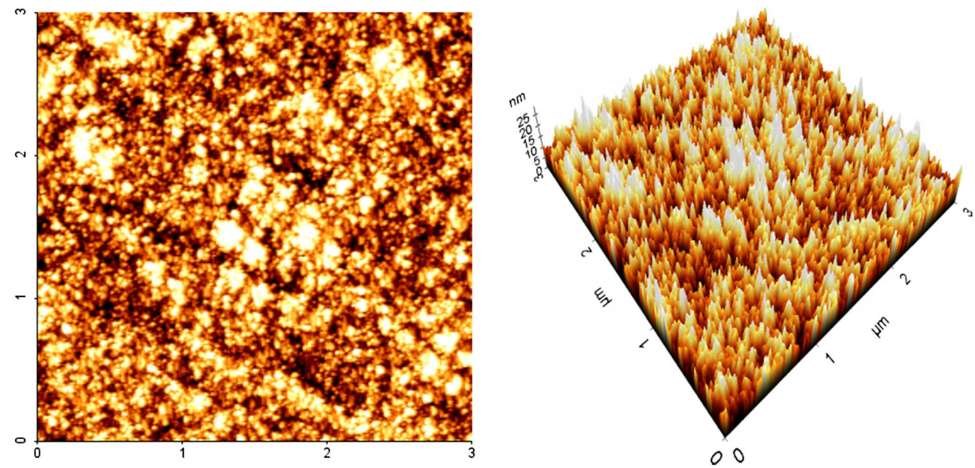

Fig. 5 AFM image of the LBMO film deposited on Si substrate

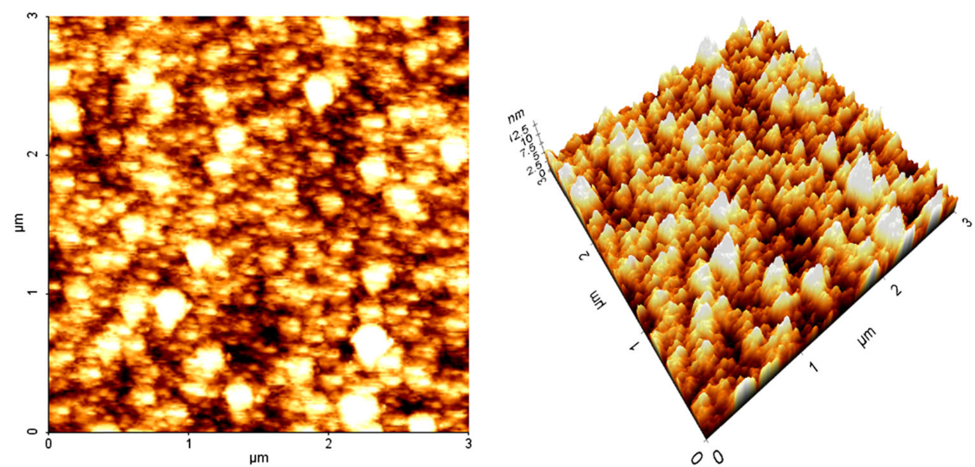

Fig. 6 AFM image of the LBMO film deposited on MgO substrate

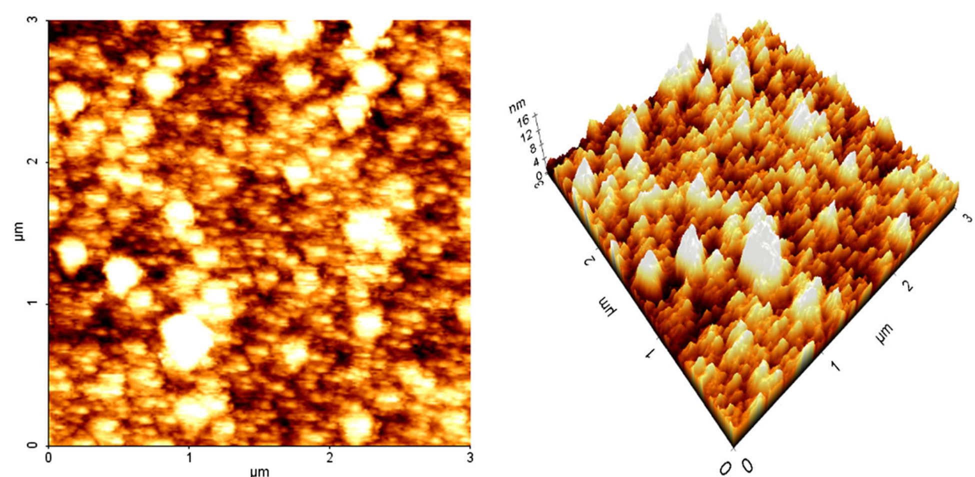

Fig. 7 AFM image of the LBMO film deposited on c-ZrO_2 substrate

contraction of the in plane lattice parameter. However, if the difference in the lattice parameter is significantly large, an island-type growth starts at the beginning of film deposition. The lattice parameter of bulk $La_{0.7}Ba_{0.3}MnO_3$ is 0.391 nm, whereas for the cubic crystals of Si, MgO, and c-ZrO_2, it is 0.5431, 0.4312, and 0.5214 nm, respectively. The obtained lattice parameters of the LBMO films are given in Table 2.

Compositional analysis

The composition of the LBMO films deposited on different substrates is analyzed by energy dispersive spectroscopy (EDS) and shown in Figs. 2, 3, 4. From figures, it was observed that the elements of La, Ba, Mn, and O were observed in the LBMO films without any impurities. All the deposited films showed nearly stoichiometric ratio.

Surface morphology

Figures 5, 6, 7 show the AFM images of the LBMO thin films deposited on Si, MgO, and c-ZrO_2 substrates. The mean roughness (RMS) of the surfaces is calculated for a 9 μm^2 scan area. It was clearly seen that both the RMS roughness and grain size of the films changed with substrate. It is found that the mean roughness of films deposited on Si, MgO, and c-ZrO_2 is 0.6, 3.4, and 4.9 nm, respectively. It is known that the change in surface roughness may cause deterioration of the electrical properties. These results, together with the XRD analysis, clearly indicated that the crystallinity is influenced by the nature of substrates.

Electrical properties

The electrical resistivity of LBMO thin films depends on the microstructural and lattice mismatch between the substrate and films. It is also observed that there is a clear change of resistivity values with changing the substrate material. The films showed high electrical resistivity of 27.8 MΩ cm when deposited on c-ZrO_2 and low electrical resistivity of 4.37 MΩ cm for the films deposited on MgO substrate. Figure 8 shows the temperature dependence of resistivity for the films deposited on different substrates. The electrical resistivity for LBMO films deposited on MgO substrate has lower resistivity with low transition temperature, whereas LBMO films deposited on Si substrate, exhibited high transition temperature nearer to the room temperature.

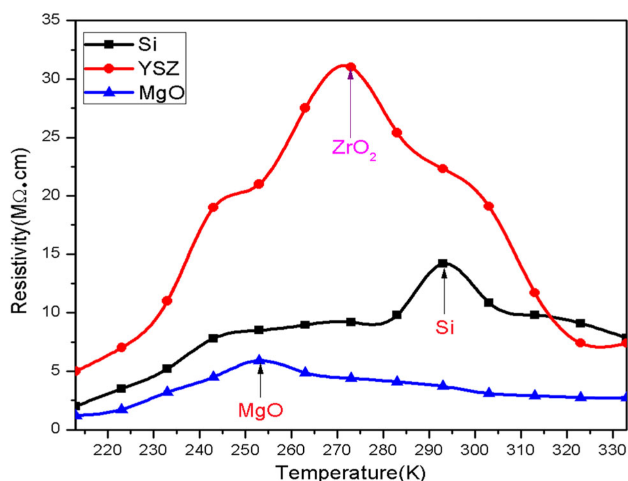

Fig. 8 Variation of electrical resistivity of LBMO films deposited on different substrates

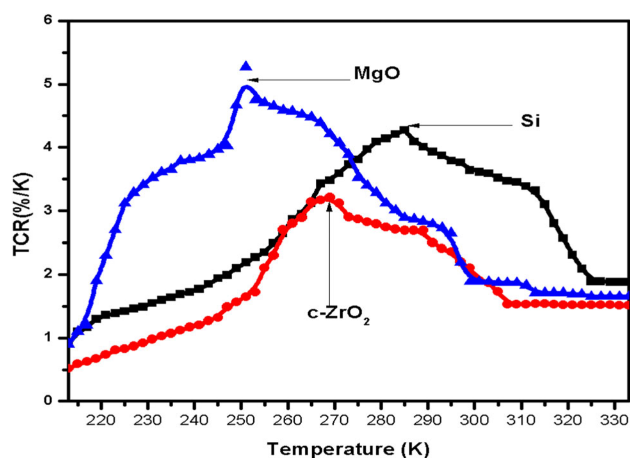

Fig. 9 Temperature dependence of TCR of LBMO films deposited on different substrates

Figure 9 shows the TCR as a function of temperature for the films deposited on Si, MgO, and c-ZrO_2substrates. The TCR values are 5.32 %/K at 245 K for the MgO sample, 4.09 %/K at 295 K for the Si sample, and 3.2 %/K at 268 K for c-ZrO_2 sample.

Conclusions

High quality thin films of LBMO have been grown on Si (100), MgO (100), and c-ZrO_2 using electron beam evaporation method for the first time The crystalline quality of all films has been analyzed and found to be excellent. The resistivities of the films varied with substrates, due to the microstructural and lattice mismatch between the substrate and films. Films prepared on MgO substrate have shown high TCR (5.32 %/K) at low transition temperature (245 K), but films deposited on Si substrate have shown better TCR (4.09 %/K) value at room temperature. From the above results, we conclude that films deposited on Si substrates were useful for uncooled bolometer applications.

Acknowledgments The authors acknowledge the financial support from the Council for Scientific and Industrial Research (Project No: 03(1173)/10/-EMR-II), New Delhi.

Open Access This article is distributed under the terms of the Creative Commons Attribution 4.0 International License (http://creativecommons.org/licenses/by/4.0/), which permits unrestricted use, distribution, and reproduction in any medium, provided you give

appropriate credit to the original author(s) and the source, provide a link to the Creative Commons license, and indicate if changes were made.

References

Antonakos A, Lampakis D, Liarokapis E, Filippi M, Prellier W, Aydogdu GH, Habermeier HU (2008) J Phys Condens Matter 20:434232

Chahara KI, Ohno T, Kasai M, Kozono Y (1993) Appl Phys Lett 63:1990

Chen CH, Cheong S-W (1996) Phys Rev Lett 76:4042

Goyal A, Rajeswari M, Shreekala R, Lofland SE, Bhagat SM, Boettcher T, Kwon C, Ramesh R, Venkate-san T (1997) Appl Phys Lett 71:2535

Helmolt RV, Weeker J, Holzapfel B, Schultz L, Samwer K (1993) Phys Rev Lett 71:2331

Hong NH, Sakai J, Noudem JG, Hassini A, Gervais M, Gervais F (2003) J Phys Condens Matter 15:6527

Huang Zh, Gao GY, Yin ZhZh, Feng XX, Chen YZh, Zhao XR, Sun JR, Wu WB (2009) J Appl Phys 105:113919

Jin S, Tiefel TH, Mc Cormack M, Fastnacht RA, Ramesh R, Chen LH (1994) Science 264:413

Jirak Z, Damay F, Hervieu M, Martin C, Raveau B, Andreé G, Boureé F (2000) Phys Rev B 61:1181

Kusters RM, Singleton J, Keen DA, McGreevy R, Hayes W (1989) Phys B 155:362

Ovsyannikov GA, Petrzhik AM, Borisenko IV, Klimov AA, Ignatov YuA, Demidov VV, Nikitov SA (2009) J Exp Theor Phys 108:48

Rajeswari M, Chen CH, Goyal A, Kwon C, Robson MC, Ramesh R, Venkatesan T, Lakeou S (1996) Appl Phys Lett 68:3555

Renner Ch, Aeppli G, Kim BG, Ah Soh Y, Cheong SW (2002) Nature 416:518

Renner Ch, Aeppli G, Ronnow HM (2005) Mater Sci Eng C 25:775

Sagdeo PR, Lalla NP, Narlika AV, Prabhakaran D, Boothroyd AT (2008) Phys Rev B 78:174106

Salamon MB, Jaime M (2001) Rev Mod Phys 73:583

Shan PC, ÇelikButler Z, Butler DP, Jahanzeb A (1995) J Appl Phys 78:7334

Tokura Y, Tomioka Y (1999) J Magn Magn Mater 200:1

Uehara M, Mori S, Chen CH, Cheong SW (1999) Nature 399:560

Vas'ko VA, Nordman CA, Kraus PA, Achutharaman VS, Ruosi AR, Goldman AM (1996) Appl Phys Lett 68:2571

Wang JZh, Sun JR, Dong QY, Liu GJ, Shen BG (2009) Solid State Commun 149:325